4.1.2.5 Prominences and ejecta

Klaus Wilhelm

4.1.2.5.1 Prominences

Prominences are structures of relatively cool material (with chromospheric temperatures) in the hot corona (cf., Sect. 4.1.1.5.2). They are supported by magnetic fields, cf., [a, c, 84Ler, 06Anz]. Whereas most of the models involve mainly horizontal magnetic field directions, evidence is presented by [98Zir] that vertical fields are required to understand the counter-streaming flows observed. The formation of a prominence condensation through localized loop heating in the chromosphere and catastrophic cooling in the corona is modelled by [99Ant2].

Prominences show a filamentary structure in H I Lyα with threads thinner than 1.5 Mm [80Bon]. The physical conditions of a quiescent prominence were studied with the help of emission lines in H I, He I, O IV, Si IV, and C IV spectra [83Pol]. For observations of an active prominence see [01Gil]. The varying appearance of a prominence with the formation temperatures of the spectral lines led to the suggestion that many flux tubes of different temperatures were involved. A helium-to-hydrogen abundance ratio of 0.1 was found by [93Lam].

The Ne VII 46.5 nm line shows absorption effects near prominences [73Tou]. Continuum absorption of other spectral lines shortwards of the H I Lyman edge at 91.2 nm have also been observed [79Sch]. The H I Lyman and the He II Balmer continua contribute to the absorption. By studying this absorption, a column density of 1×10^{18} cm^{-2} of hydrogen in a prominence, and a filling factor greater than ≈ 0.3 was obtained [98Kuc]. From studies of the Lyman continuum, electron temperatures between 7500 K and 8300 K were deduced [05Par]. Spacecraft data of the H I Lyman series, the He I lines at 53.7 nm and 58.4 nm, and ground-based observations showed a cool prominence body with $T_e < 1 \times 10^4$ K, surrounded by hotter layers with temperatures of $\approx 6 \times 10^4$ K. The corresponding non-thermal velocities are ≈ 4 km s^{-1} and ≈ 20 km s^{-1}, respectively [98deB, 03Dam].

Spectra of the H I Lyman and Balmer lines of several prominences have been obtained by [01Hei2, 03Ste, 05Ste]. No self-reversals of the Lyman lines with series numbers higher than Lyα were found in one prominence, whereas, in other cases, all lines had rather strong reversals, suggesting that the prominence-corona transition region is seen along the magnetic field in the first case and across in the second case. As an example the spectrum near the H I Lyman edge is shown in Fig. 1.

Jet observations in He II 30.4 nm [99Wan, 01Wan] indicated that even quiescent prominences are of a dynamic nature, with plasma speeds of ≈ 30 km s^{-1}. This is consistent with the findings that spectral lines formed at transition-region temperature indicate high line-of-sight (LOS) velocities (≈ 20 km s^{-1}) in prominences [77Mei, 97Wil, 02Wil1].

Spectral atlasses of prominences have been prepared in the wavelength ranges from 133.5 nm to 167 nm by [d], and from 80 nm to 160 nm by [f]. A prominence appears to contain hotter material at lower than at greater heights. The spectral observations confirm earlier results by [77Fel, 79Mar, 97Wil] that the line widths in a prominence are narrower than in quiet-Sun areas.

A book on the nature of solar prominences by [g] and a recent review of prominence science with emphasis on recent results by [02Pat] cover this subject.

4.1.2.5.2 Filaments

Filaments and prominences are two aspects of the same phenomenon. Filaments are observed on the disk and prominences above the limb. The H I Lyman continuum absorption suppresses the transition-region emission and makes the filament discernible in this range. A filament is much more extended in extreme-ultraviolet (EUV) radiation than in Hα [01Hei1, 01Chi, 04Sch, 04Del, 06Sch].

Models involving twisted magnetic fields in a dip configuration to support this material have been presented by [06Anz]. Filament oscillations were studied by [04Oka].

4.1.2.5.3 Eruptive prominences, filaments, and coronal mass ejections

Eruptive prominences and filaments are more closely related to Coronal Mass Ejections (CME) than active prominences [00Gil]. A spectrum of an erupting prominence in the wavelength range from 30 nm to 63 nm was observed by [86Wid]. The eruption was associated with a large flare and showed emissions in O IV, O V and Ne VII, in addition to He I and He II. An eruptive prominence was also studied by [89Fon]. In this case, the plasma was heated to transition-region temperatures with almost no cool core left. No CME followed, but the electron density in the corona above the prominence was reduced. A clear coronal dimming in X-ray fluxes associated with a large prominence eruption was observed by [98Gop1]. CMEs with interesting helical structures were seen, interpreted as magnetic flux ropes [89Der, 99Woo, 00Cia]. A twisted magnetic flux rope model as cause of CMEs and two-ribbon flares (cf., Sect. 4.1.2.7) has been presented by [00Ama]. Flux-rope models for a CME following an erupting prominence have also been suggested by [00McA, 02Yur] based on spacecraft and ground observations. A similar model was discussed more than 20 years ago by [78Mou]. Multi-polar topologies and reconnection between sheared flux systems triggers an eruption according to [99Ant1]. Recent observations of CMEs and the accompanying events are listed in Table 1. Only a limited selection of articles could be included with emphasis on multi-wavelength measurements. In the near future, CME observations with the help of the two *STEREO*[1] spacecraft will be of importance, but they could not yet be taken into account here.

Most of the CMEs were observed with white-light coronagraphs. A comparison of ground-based and spacecraft CME observations in the 1980's has been performed by [99StC], more recent results are reviewed by [06Pic], confirming the general three-part structure of CMEs: a bright leading edge, followed by a dark cavity, and a post-eruption brightening. A study of CME sizes

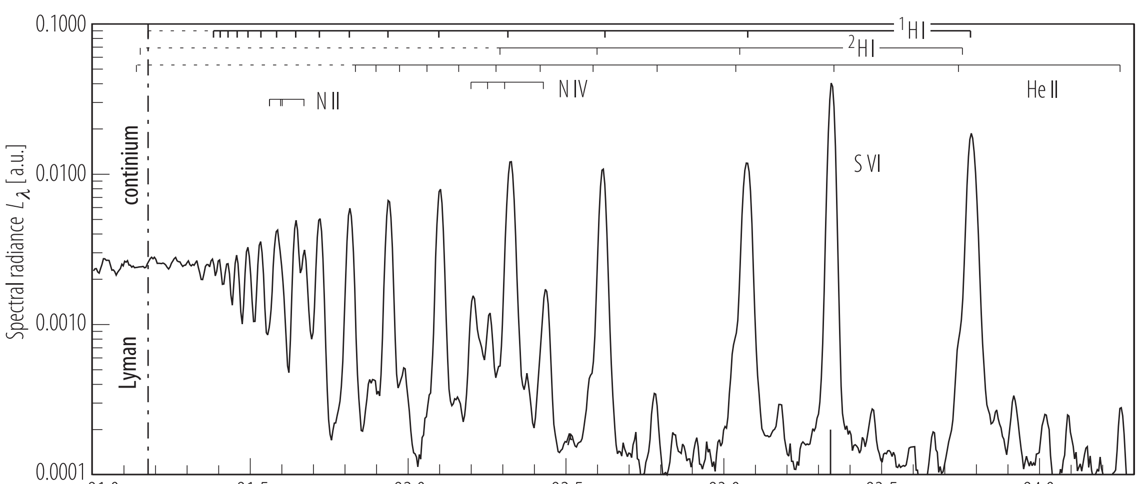

Fig. 1. Vacuum-ultraviolet spectrum with the high members of the H I Lyman series (Ly 5 to Ly 20) and the edge of the Lyman continuum observed in a solar prominence on 25 June 1996. In addition, some He II Balmer lines (in the range He II Ba 10 to Ba 22) can be seen, but deuterium lines cannot be detected. The theoretical wavelength positions of the lines and the continuum edges of hydrogen, deuterium and He^+ are indicated together with some prominent emission lines of N I, N II and S VI [04Wil].

[1] *Solar* TErrestrial *RElations Observatory*

and locations is presented in [93Hun]. An estimated mass loss of $\approx 1 \times 10^{11}$ kg is a typical value for CMEs. The influence of projection effects on the determination of CME properties was considered by [04Bur] Gradual CMEs with balloon-like shapes and impulsive CMEs – often associated with flares – have been identified by [99She]. Coronal EUV dimmings are seen in association with CMEs [97Ste, 99Zar, 00Tho, 00Har, 03Har]. Spectral observations in many emission lines allowed the conclusion that the coronal dimming is caused by mass loss of the corona and not by temperature variations.

A halo CME, which originated from the centre of the solar disk and travelled to the Earth, was related to a "sigmoid" structure in soft X-ray emission [00Ste2]. The S-shaped structures along neutral lines were most prominent at temperatures of 2.4 MK, but much weaker or absent at lower temperatures. A very strong Earth-directed CME occurred in May 1997 [98Tho]. Such halo events cause, in general, geomagnetic storms and are thus important for space weather predictions [00Web]. The signatures of CMEs near the Sun and the resulting magnetic cloud travelling in the interplanetary medium are compared by [98Gop2].

Flares and CMEs are closely related, but do not drive one another [95Har] (cf., Sect. 4.1.2.7). The initial phase of CMEs occurs before the onset of an associated flare, which coincides, however, with the acceleration phase of the CME [01Zha]. The relation between flares and CMEs was also studied by [03Zha]. Fast CMEs are associated with two-ribbon brightenings during the flare, whereas slow CMEs sometimes show tubular emission. A series of six recurrent flares and halo CMEs occurred in from 24 to 26 November 2000 [04Che]. Flare and CME onsets with expansion speeds of up to 650 km s^{-1} of the 10 MK plasma have been recorded by [01Inn]. A shock wave is thought to heat and accelerate the loop structure. CMEs associated with X-class flares contained no cool prominence material, but the O VI lines at 103.2 nm and 103.7 nm showed a splitting indicative of LOS velocities of ± 800 km s^{-1} [03Ray]. Reviews of the physical principle related to CMEs are provided by [00For, 01Low]. A picture of CMEs has been developed by [06Spi] that compares the solar flare process to a substorm in the Earth's magnetosphere and ionosphere.

4.1.2.5.4 Spicules and macrospicules

Spicule observations and theoretical concepts of the spicule formation have been reviewed by [00Ste1]. Their small sizes and short lifetimes place severe constraints on the observations required to conceive a satisfactory spicule model. Spicules with Doppler LOS velocities of up to ± 30 km s^{-1} are shown in Fig. 2 as observed by SUMER on SOHO. The average downflow in the transition region was explained by [78Pne] as a return flow of spicular material. In all likelihood, the transition-region spicules are outward extensions of chromospheric spicules [87Der]. Disk spicules seen in the wings of Hα exhibit upward and downward velocities in such a way that the entire spicular plasma rises and falls as a whole [95Sue].

Time series of spicules and macrospicules have been studied by [05Xia]. "Falling after rising" material in some of the spicules could be seen, and recurrent events within five to six minutes. Spicules observed in various VUV emission lines, which are formed at temperatures between 3×10^4 K and 6×10^5 K, exhibited an increase in their diameters with growing temperature. Above 6×10^5 K the spicule signature is no longer discernible [98Bud]. Although the LOS geometry near the limb is not very advantageous for the observation of vertical motions, VUV observations of spicules near the poles showed significant red and blue Doppler shifts as characteristic features. This is difficult to reconcile with spicule models that are based on field-aligned propagation of material on vertical magnetic fields, and favoured a sling-shot effect [00Wil]. However, observations of the Hanle and Zeeman effects and theoretical modelling gave inclined magnetic field directions of $\approx 35^o$ and ≈ 1 μT at a height of 2000 km in spicules [05Tru]. Using Hα observations, similar tilt angles and axial velocities of about 40 km s^{-1} have been reported by [92Her].

Macrospicules were discovered by [75Boh] in He II 30.4 nm spectroheliograms of a slitless spectrograph. They had lengths of up to 50$''$ and lifetimes between 5 min and 40 min. Their occurrence

Table 1. Observations of selected coronal mass ejections (CME) described in the recent literature (in chronological order).

Date	Type	Observations[a]	Flare class[b]	Instruments[c], Spacecraft[d]	Reference
05 Apr 1994	Prominence eruption	WL; 17 GHz; SXR		NORH; SXT; LASCO; EIT	[98Gop1]
01 May 1996	Prominence eruption	VUV; WL Ca II; SXR		SUMER; CDS; EIT; LASCO; SXT; MSH	[97Wii]
31 May 1997	Filament eruption	VUV; WL Hα		EIT; SUMER; CDS; LASCO; MSDP	[00Sch]
02 May 1998	Halo	WL; Hα; 17.1 nm		EIT; LASCO	[01Poh]
09 May 1999	Limb	VUV; SEP		ERNE; SUMER	[01Tor]
11 Aug 1999	Limb	17.1 nm; 19.5 nm; 30.4 nm;		LASCO; EIT	[04Kou]
06 Jun 2000	Halo; filament eruption	B; WL	X2.3	BBSO; MDI	[05Den]
28 Feb 2001	Halo; filament eruption	VUV, B SXR		EIT; CDS; MDI; LASCO; SXT	[07Ste]
19 Oct 2001	Filament eruption	Hα dimming; 17.1 nm	X1.6	*TRACE*; EIT	[03Jia]
17 Nov 2001	Filament eruption	3.75 GHz; 17 GHz; 34 GHz; WL; SXR	M2.8	NORH; EIT; LASCO; SXI	[04Kun]
21 Apr 2002	Limb	VUV; WL SXR	X1.5	UVCS; LASCO; *TRACE*;*RHESSI*	[03Ray]
13 May 2005	Halo	Hα; WL; 17.1 nm; SXR; HXR	M8.0	*RHESSI*; SXI; *TRACE*	[07Liu]
09 Sep 2005	Halo	WL; B	X6.2	LASCO; MDI; MLSO	[06Wan]

[a] WL – White Light; SXR – Soft X Rays (100 eV to 10 keV, cf., Sect. 4.1.1.3); VUV – Vacuum UltraViolet; SEP – Solar Energetic Particles; B – Magnetic field; HXR – Hard X Rays (10 keV to 100 keV, cf. [e])
[b] X-ray flux classification [b] (as given in the reference from *GOES* observations)
[c] NORH – NObeyama RadioHeliograph; SXT – Soft X-ray Telescope on *Yohkoh*; LASCO – Large Angle Spectroscopic COronagraph on *SOHO*; EIT –Extreme-ultraviolet Imaging Telescope on *SOHO*; SUMER – Solar Ultraviolet Measurements of Emitted Radiation on *SOHO*; CDS – Coronal Diagnostic Spectrometer on *SOHO*; MSH – Meudon SpectroHeliograph; MSDP – Multi-channel Subtractive Double Spectrograph; ERNE – Energetic and Relativistic Nuclei and Electron instrument on *SOHO*; BBSO – Big Bear Solar Observatory; MDI – Michelson Doppler Imager on *SOHO*; SXI – Soft X-ray Imager on *GOES*; UVCS – UltraViolet Coronagraph Spectrometer on *SOHO*; MLSO – Mauna Loa Solar Observatory; [d] GOES – Geostationary Operational Environmental Satellites (See GOES data at `http://www.goes.noaa.gov/`.); RHESSI – Ramaty High-Energy Solar Spectroscopic Imager; TRACE – Transition Region and Coronal Explorer; SOHO – Solar and Heliospheric Observatory

is restricted to polar coronal holes, and the inclination decreases away from the poles in close resemblance to the orientation of polar plumes (cf., Sect. 4.1.1.5.2.5). Both features appear to be controlled by the diverging magnetic field of the polar caps. Macrospicules observed in Hα and in He II 30.4 nm by [98Wan] showed that all He II events had counterparts in Hα, but many Hα macrospicules are not accompanied by a corresponding He II event. Evidence is presented by [06Mad] that some blinkers (cf., Sect. 4.1.1.5.1.3) are the counterparts of He II macrospicules. A

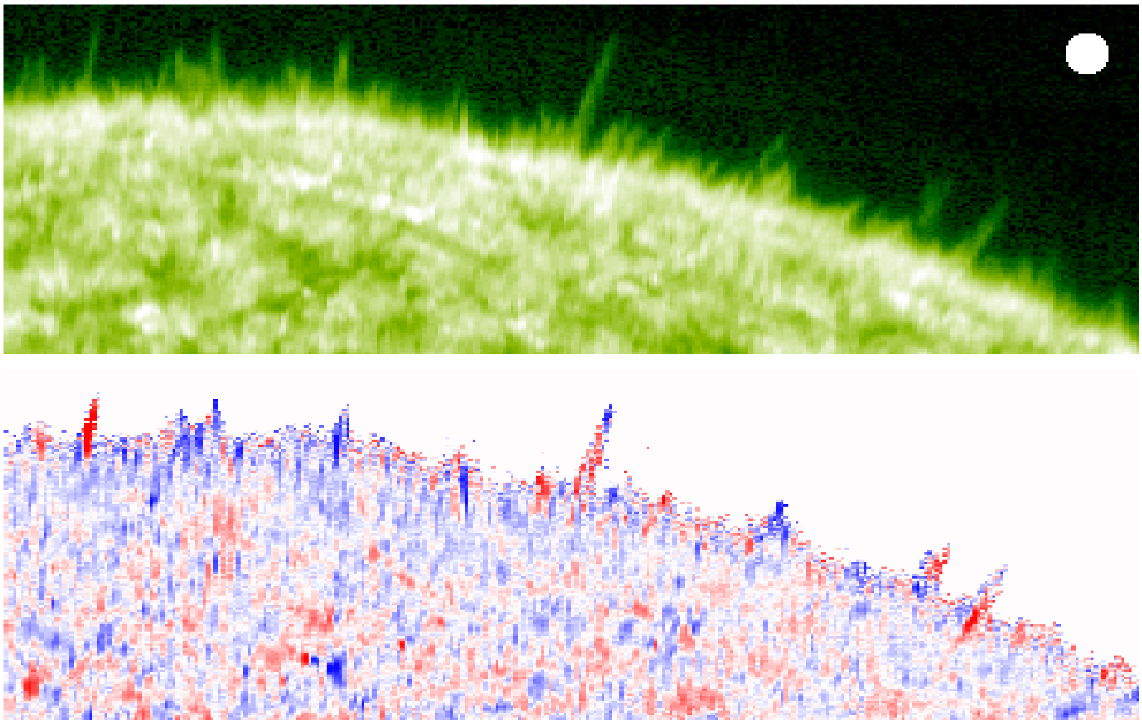

Fig. 2. (see color-picture part, page 617) Spicule activity at the solar limb in O V emission at 62.973 nm with the corresponding Doppler diagram in the lower panel. The frame dimensions are 310 Mm × 100 Mm. The tallest feature protrudes approximately 40 Mm from the limb and is a macrospicule judged by its length. The size of the Earth is shown for comparison in the upper panel [92].

distinction between polar surges and macrospicules has been proposed by [99Geo]; surges have a complex structure, whereas macrospicules are simple spikes.

A macrospicule observation in April 1996 involved high LOS velocities reaching a plateau of 200 km s^{-1} at an altitude of about 18 Mm [97Pik]. Several events with characteristics of macrospicules show Doppler shifts indicating a rotational motion [98Pik]. Electron densities of the order of 10^{10} cm^{-3} and a temperature of $\leq 3 \times 10^5$ K have to be compared with parameters in the background plasma of 1×10^8 cm^{-3} and ≈ 1 MK. The outflow speed near the limb was ≥ 80 km s^{-1} [02Par].

4.1.2.5.5 Jets and tornadoes

Jets in the corona have been discovered in high-resolution observations with a tandem Wadsworth spectrograph [83Bru]. Coronal X-ray jets in association with bright-point activity were found by [92Shi, 96Shi], and interpreted as reconnection between newly emerging magnetic flux and pre-existing coronal fields.

Spectroscopic measurements in an O V emission line showed a plasma ejection (associated with a flare and a CME) with an outward flow at a speed of ≈ 150 km s^{-1} and a superimposed rotational motion with a speed of ± 350 km s^{-1} [02Pik]. On a smaller scale, a rotational event was observed by [02Wil2]. A coronal jet was observed in a wide altitude range by [05Ko]. A fan-like jet in Mg X followed by a rotating jet seen in O V was observed at the limb by [01Har]. Speeds of ≈ 380 km s^{-1} (red) and ≈ 190 km s^{-1} (blue) were measured with indications of an acceleration. Magnetic reconnection of low-lying loops with open field lines were proposed as explanation. The spectroscopic signatures of rotating structures have thoroughly been studied by [75Rom].

Chromospheric jets seen in the C I lines near 156 nm and 166 nm have extremely fine structures and show strong red and blue Doppler shifts [83Der, 83Bru]. Inclined streaks in spectra of the C IV 154.8 nm emission line indicate local acceleration of plasma along its propagation path in the transition region. Typical accelerations are between 10 km s^{-2} and 20 km s^{-2} [02Wil2]. In close neighbourhood of this activity rotating events and coronal jets with LOS velocities of more than 200 km s^{-1} have been observed.

4.1.2.5.6 References for 4.1.2.5

Catalogues and monographs

a Bruzek, A.: Landolt-Börnstein, NS, Vol. VI/2a, Astronomy and Astrophysics (K. Schaifers, H.H. Voigt, eds.), Berlin, Heidelberg, New York: Springer-Verlag (1981) p. 120.
b Bruzek, A.: Landolt-Börnstein, NS, Vol. VI/2a, Astronomy and Astrophysics (K. Schaifers, H.H. Voigt, eds.), Berlin, Heidelberg, New York: Springer-Verlag (1981) p. 124.
c Durrant, C.J.: Landolt-Börnstein, NS, Vol. VI/3a, Astronomy and Astrophysics (H.H Voigt, ed.), Berlin, Heidelberg, New York: Springer-Verlag (1993) p. 101.
d Engvold, O., Hansteen, V., Kjeldseth-Moe, O., Brueckner, G.E.: Astrophys. Space Sci. **170** (1990) 179.
e ISO 21348: 2007 Space Environment (Natural and Artificial) – Process for Determining Solar Irradiances, Genève, International Organization for Standardization (2007).
f Parenti, S., Vial, J.-C., Lemaire, P.: Astron. Astrophys. **443** (2005) 679.
g Tandberg-Hanssen, E.: The Nature of Solar Prominences, Astrophys. Space Sci. Library **199** Dordrecht: Kluwer (1995).

Special references

73Tou Tousey, R., Bartoe, J.-D.F., Bohlin, J.D., et al.: Sol. Phys. **33** (1973) 265.
75Boh Bohlin, J.D., Vogel, S.N., Purcell, J.D., et al.: Astrophys. J. **197** (1975) L133.
75Rom Rompolt, B.: Sol. Phys. **41** (1975) 329.
77Fel Feldman, U., Doschek, G.A.: Astrophys. J. **216** (1977) L119.
77Mei Mein, P.: Sol. Phys. **54** (1977) 45.
78Mou Mouschovias, T., Poland, A.I.: Astrophys. J. **220** (1978) 672.
78Pne Pneuman, G.W., Kopp, R.A.: Sol. Phys. **57** (1978) 49.
79Mar Mariska, J.T., Doschek, G.A., Feldman, U.: Astrophys. J. **232** (1979) 929.
79Sch Schmahl, E.J., Orrall, F.Q.: Astrophys. J. **231** (1979) L41.
80Bon Bonnet, R.M., Bruner, E.C., Jr., Acton, L.W., et al.: Astrophys. J. **237** (1980) L47.
83Bru Brueckner, G.E., Bartoe, J.-D.F.: Astrophys. J. **272** (1983) 329.
83Der Dere, K.P., Bartoe, J.-D.F., Brueckner, G.E.: Astrophys. J. **267** (1983) L65.
83Pol Poland, A.I., Tandberg-Hanssen, E.: Sol. Phys. **84** (1983) 63.
84Ler Leroy, J.L., Bommier, V., Sahal-Brechot, S.: Astron. Astrophys. **131** (1984) 33.
86Wid Widing, K.G., Feldman, U., Bhatia, A.K.: Astrophys. J. **308** (1986) 982.
87Der Dere, K.P., Bartoe, J.-D.F., Brueckner, G.E., et al.: Sol. Phys. **114** (1987) 223.
89Der Dere, K.P., Bartoe, J.-D.F., Brueckner, G.E., Recely, F.: Astrophys. J. **345** (1989) L95.
89Fon Fontenla, J.M., Poland, A.I.: Sol. Phys. **123** (1989) 143.
92Her Heristchi, D., Mouradian, Z.: Sol. Phys. **142** (1992) 21.
92Shi Shibata, K., Nozawa, S., Matsumoto, R.: PASJ **44** (1992) 265.

93Hun Hundhausen, A.J.: J. Geophys. Res. **98** (1993) 13177.
93Lam Laming, J.M., Feldman, U.: Astrophys. J. **403** (1993) 434.
95Har Harrison, R.A.: Astron. Astrophys. **304** (1995) 585.
95Sue Suematsu, Y., Wang, H., Zirin, H.: Astrophys. J. **450** (1995) 411.
96Shi Shibata, K., Yokoyama, T., Shimojo, M.: Adv. Space Res. **17** (1996) 197.
97Pik Pike, C.D., Harrison, R.A.: Sol. Phys. **175** (1997) 457.
97Ste Sterling, A.C., Hudson, H.S.: Astrophys. J. **491** (1997) L55.
97Wii Wiik, J.E., Schmieder, B., Kucera, T., et al.: Sol. Phys. **175** (1997) 411.
97Wil Wilhelm, K., Lemaire, P., Curdt, W., et al.: Sol. Phys. **170** (1997) 75.
98Bud Budnik, F., Schröder, K.-P., Wilhelm, K., Glassmeier, K.-H.: Astron. Astrophys. **334** (1998) L77.
98deB de Boer, C.R., Stellmacher, G., Wiehr, E.: Astron. Astrophys. **334** (1998) 280.
98Gop1 Gopalswamy, N., Hanaoka, Y.: Astrophys. J. **498** (1998) 179.
98Gop2 Gopalswamy, N., Hanaoka, Y., Kosugi, T., et al.: Geophys. Res. Lett. **25** (1998) 2485.
98Kuc Kucera, T.A., Andretta, V., Poland, A.I.: Sol. Phys. **183** (1998) 107.
98Pik Pike, C.D., Mason, H.E.: Sol. Phys. **182** (1998) 333.
98Tho Thompson, B.J., Plunkett, S.P., Gurman, J.B., et al.: Geophys. Res. Lett. **25** (1998) 2465.
98Wan Wang, H.: Astrophys. J. **509** (1998) 461.
98Zir Zirker, J.B., Engvold, O., Martin, S.F.: Nature **396** (1998) 440.
99Ant1 Antiochos, S.K., DeVore, C.R., Klimchuk, J.A.: Astrophys. J. **510** (1999) 485.
99Ant2 Antiochos, S.K., MacNeice, P.J., Spicer, D.S., Klimchuk, J.A.: Astrophys. J. **512** (1999) 985.
99Geo Georgakilas, A.A., Koutchmy, S., Alissandrakis, C.E.: Astron. Astrophys. **341** (1999) 610.
99She Sheeley, N.R., Walters, J.H., Wang, Y.-M., Howard, R.A.: J. Geophys. Res. **104** (1999) 24739.
99StC St.Cyr, O.C., Burkepile, J.T., Hundhausen, A.J., Lecinski, A.R.: J. Geophys. Res. **104** (1999) 12493.
99Wan Wang, Y.-M.: Astrophys. J. **520** (1999) L71.
99Woo Wood, B.E., Karovska, M., Chen, J., et al.: Astrophys. J. **512** (1999) 484.
99Zar Zarro, D.M., Sterling, A.C., Thompson, B.J., et al.: Astrophys. J. **520** (1999) L139.
00Ama Amari, T., Luciani, J.F., Mikic, Z., Linker, J.: Astrophys. J. **529** (2000) L49.
00Cia Ciaravella, A., Raymond, J.C., Thompson, B.J., et al.: Astrophys. J. **529** (2000) 575.
00For Forbes, T.G.: J. Geophys. Res. **105** (2000) 23153.
00Gil Gilbert, H.R., Holzer, T.E., Burkepile, J.T., Hundhausen, A.J.: Astrophys. J **537** (2000) 503.
00Har Harrison, R.A., Lyons, M.: Astron. Astrophys. **358** (2000) 1097.
00McA McAllister, H., Martin, S.F.: Adv. Space Res. **26** (2000) 469.
00Sch Schmieder, B., Delannée, C., Yong, D.Y., et al.: Astron. Astrophys. **358** (2000) 728.
00Ste1 Sterling, A.C.: Sol. Phys. **196** (2000) 79.
00Ste2 Sterling, A.C., Hudson, H.S., Thompson, B.J., Zarro, D.M.: Astrophys. J. **532** (2000) 628.
00Tho Thompson, B.J., Cliver, E.W., Nitta, N., et al.: Geophys. Res. Lett. **27** (2000) 1431.
00Web Webb, D.F., Cliver, E.W., Crooker, N.U., et al.: J. Geophys. Res. **105** (2000) 7491.
00Wil Wilhelm, K.: Astron. Astrophys. **360** (2000) 351.
01Chi Chiuderi Drago, F., Alissandrakis, C.E., Bastian, T., et al.: Sol. Phys. **199** (2001) 115.
01Gil Gilbert, H.R., Serex, E.C., Holzer, T.E., et al.: Astrophys. J. **550** (2001) 1093.
01Har Harrison, R.A., Bryans, P., Bingham, R.: Astron. Astrophys. **379** (2001) 324.
01Hei1 Heinzel, P., Schmieder, B., Tziotziou, K.: Astrophys. J. **561** (2001) 223.
01Hei2 Heinzel, P., Schmieder, B., Vial, J.-C., Kotrč, P.: Astron. Astrophys. **370** (2001) 281.

01Inn Innes, D.E., Curdt, W., Schwenn, R., et al.: Astrophys. J. **549** (2001) L249.
01Low Low, B.C.: J. Geophys. Res. **106** (2001) 25141.
01Poh Pohjolainen, S., Maia, D., Pick, M., et al.: Astrophys. J. **556** (2001) 421.
01Tor Torsti, J., Kocharov, L., Innes, D.E., et al.: Astron. Astrophys. **365** (2001) 198.
01Wan Wang, Y.-M.: Astrophys. J. **560** (2001) 456.
01Zha Zhang, J., Dere, K.P., Howard, R.A., et al.: Astrophys. J. **559** (2001) 452.
02Par Parenti, S., Bromage, B.J.I., Bromage, G.E.: Astron. Astrophys. **384** (2002) 303.
02Pat Patsourakos, S., Vial, J.-C.: Sol. Phys. **208** (2002) 253.
02Pik Pike, C.D., Mason, H.E.: Sol. Phys. **206** (2002) 359.
02Wil1 Wilhelm, K., Inhester, B., Newmark, J.S.: Astron. Astrophys. **382** (2002) 328.
02Wil2 Wilhelm, K., Dammasch, I.E., Hassler, D.M.: Astrophys. Space Sci. **282** (2002) 189.
02Yur Yurchyshyn, V.B.: Astrophys. J. **576** (2002) 493.
03Dam Dammasch, I.E., Stellmacher, G., Wiehr, E.: Astron. Nachr. **324** (2003) 338.
03Har Harrison, R.A., Bryans, P., Simnett, G.M., Lyons, M.: Astron. Astrophys. **400** (2003) 1071.
03Jia Jiang, Y., Ji, H., Wang, H., Chen, H.: Astrophys. J. **597** (2003) L161.
03Ray Raymond, J.C., Ciaravella, A., Dobrzycka, D., et al.: Astrophys. J. **597** (2003) 1106.
03Ste Stellmacher, G., Wiehr, E., Dammasch, I.E.: Sol. Phys. **217** (2003) 133.
03Zha Zhang, M., Golub, L.: Astrophys. J. **595** (2003) 1251.
04Bur Burkepile, J.T., Hundhausen, A.J., Stanger, A.L., et al.: J. Geophys. Res. **109** (2004) A03103.
04Che Chertok, I.M., Grechnev, V.V., Hudson, H.S., Nitta, N.V.: J. Geophys. Res. **109** (2004) A02112.
04Del Del Zanna, G., Chiuderi Drago, F., Parenti, S.: Astron. Astrophys. **420** (2004) 307.
04Kou Koutchmy, S., Baudin, F., Bocchialini, K.: Astron. Astrophys. **420** (2004) 709.
04Kun Kundu, M.R., White, S.M., Garaimov, V.I., et al.: Astrophys. J. **607** (2004) 530.
04Oka Okamoto, T.J., Nakai, H., Keiyama, A., et al.: Astrophys. J. **608** (2004) 1124.
04Sch Schmieder, B., Lin, Y., Heinzel, P., Schwartz, P.: Sol. Phys. **221** (2004) 297.
04Wil Wilhelm, K., Dwivedi, B.N., Marsch, E., Feldman, U.: Space Sci. Rev. **111** (2004) 415.
05Den Deng, N., Liu, C., Yang, G., et al.: Astrophys. J. **623** (2005) 1195.
05Ko Ko, Y.-K., Raymond, J.C., Gibson, S.E., et al.: Astrophys. J. **623** (2005) 519.
05Par Parenti, S., Lemaire, P., Vial, J.-C.: Astron. Astrophys. **443** (2005) 685.
05Ste Stellmacher, G., Wiehr, E.: Astron. Astrophys. **431** (2005) 1069.
05Tru Trujillo Bueno, J., Merenda, L., Centeno, R., et al.: Astrophys. J. **619** (2005) 191.
05Xia Xia, L., Popescu, M.D., Doyle, J.G., Giannikakis, J.: Astron. Astrophys. **438** (2005) 1115.
06Anz Anzer, U., Heinzel, P.: Astron. Astrophys. **446** (2006) 301.
06Mad Madjarska, M.S., Doyle, J.G., Hochedez, J.-F., Theissen, A.: Astron. Astrophys. **452** (2006) L11.
06Pic Pick, M., Forbes, T.G., Mann, G., et al.: Space Sci. Rev. **123** (2006) 341.
06Sch Schwartz, P., Heinzel, P., Schmieder, B., Anzer, U.: Astron. Astrophys. **459** (2006) 651.
06Spi Spicer, D.S., Sibeck, D., Thompson, B.J., Davila, J.M.: Astrophys. J. **643** (2006) 1304.
06Wan Wang, Y., Xue, X., Shen, C., et al.: Astrophys. J. **646** (2006) 625.
07Liu Liu, C., Lee, J., Yurchyshyn, V., et al.: Astrophys. J. **669** (2007) 1372.
07Ste Sterling, A.C., Harra, L.K., Moore, R.L.: Astrophys. J. **669** (2007) 1359.